Proceedings of the Eighth Asian Congress of Fluid Mechanics
December 6-10, 1999, Shenzhen, China

REVIEW OF COMPRESSIBLE DYNAMIC STALL AND ITS CONTROL

M.S.Chandrasekhara
(Navy-NASA Joint Institute of Aeronautics, Department of Aeronautics and Astronautics
Naval Postgraduate School, Monterey, CA, 93943, USA)

ABSTRACT: A review of compressibility effects on dynamic stall of pitching airfoils and unsteady separation control by manipulation of unsteady vorticity using a deformable leading edge airfoil design is presented.

I. INTRODUCTION

Dynamic stall is important to helicopters, pitching aircraft, wind turbines and turbomachinery. It is associated with the production of unsteady lift by rapidly pitching an airfoil past the static stall angle. The dynamic lift generated by the airfoil can be twice its maximum steady lift. This is attributable to the large amount of coherent vorticity and hence circulation, produced due to the unsteady pitching motion. A dynamic stall vortex abruptly forms near the leading edge, when the local vorticity level exceeds an unknown critical value. This occurs over a very small angle of attack range ($O(0.5^o)$). The vortex convects over the airfoil, during which process a very strong, undesirable, nose down pitching moment is induced. Usually moment stall occurs prior to lift stall caused by vortex shedding (Ref. 1). Complicating matters is the fact that even at very low freestream speeds ($M_\infty = 0.3$), the high angles of attack of the airfoil cause the local flow to become supersonic and eventually form shocks. These factors combine to accelerate dynamic stall onset, leading to a rapid loss of lift at progressively decreasing angles of attack with increasing compressibility effects.

The mechanisms of compressible dynamic stall onset are very sensitive to the Reynolds number and Mach number of the flow and can change depending on whether the airfoil is tripped or not. Three different mechanisms have been identified and discussed in Ref. 2.

1. The bursting of a laminar separation bubble at low Reynolds number ($< 1x10^6$) and Mach number (< 0.35)
2. Shock induced separation at high Reynolds number ($> 1.5x10^6$) and Mach number (> 0.4). In both cases, large values of leading edge adverse pressure gradient are involved.
3. Interactions between the laminar bubble and the supersonic flow that rides over it at *very low* adverse pressure gradient for intermediate conditions. It can be changed to the pressure gradient type by simply tripping the airfoil.

Ref. 3 shows that the vorticity flux in the flow is related to the adverse pressure gradient as follows:

$$\nu\frac{\partial\Omega}{\partial n} = \frac{\partial U_S}{\partial t} + \frac{1}{\rho}\frac{\partial p}{\partial s} + V\Omega$$

Here, the LHS is the vorticity flux, the first term on the RHS is the unsteady surface acceleration, the second, the potential flow pressure gradient. The last term, the surface transpiration, is important when the flow is controlled using suction or injection. It is clear that control of dynamic stall requires manipulation of the flow vorticity field. In the absence of surface mass injection, it appears that the key to compressible dynamic stall control lies in controlling the leading edge adverse pressure gradient. However, the fixed geometry of the wing or airfoil makes it normally

impossible. Hence, a dynamically deforming leading edge airfoil was designed to actively change the airfoil profile and hence, the potential flow distribution over it, to control flow separation. This paper describes an approach where the airfoil is adapted to the instantaneous flow condition in order to maintain attached flow to higher than usual angles of attack. The dynamic wing adaptation introduces an additional unsteady surface acceleration term in the above equation. Thus, this flow is characterized by two independent time scales, and depending on their relative phasing, stall can even be promoted.

II. DESCRIPTION OF THE EXPERIMENT

The dynamically deforming leading edge airfoil is a 6-inch chord, NACA 0012 airfoil when the leading edge is fully extended. The first 20% of the DDLE airfoil is made from a carbon-fiber composite skin, which is attached to the rest of the (solid aluminum) airfoil at one end. At the other end, the skin is held by a tang to a truss/mandrel combination, placed *inside* the airfoil. An a.c. brushless servomotor is used to drive the mandrel from each side of the test section. Rapid deformation rates are possible with this design. The deformation to a semicircular leading edge (a 320% change in the nose curvature) can be completed in 15 ms and just 0.08in movement, at M_∞ = 0.4. In actual use, since an intermediate maximum curvature is selected, the displacement required is significantly smaller, $\approx$ 0.025in or less. Fig. 1 (Ref. 4) shows the construction details of the DDLE airfoil. The various airfoil profiles are categorized into shape numbers, with the NACA 0012 profile as shape-0 and the semicircular nose profile as shape-27. Each 0.003in retraction of the leading edge corresponds to an integer increase in shape number. The airfoil deformation schedule (rate of change of leading edge curvature, the angle of attack at which it is initiated and terminated, the dwell time at any shape, etc.) is fully controllable.

The experiments were conducted in the Navy-NASA Joint Institute of Aeronautics Compressible Dynamic Stall Facility (CDSF). The CDSF is an in-draft wind tunnel with a 14in x 10in test section, operated by a continuously running evacuation compressor. The airfoil is oscillated sinusoidally using an electro-mechanical drive system. The speed range of the CDSF and the oscillation parameters are: $0 \le M_\infty \le 0.5$, $0^\circ \le \alpha_{mean} \le 15^\circ$, $2^\circ \le \alpha_{amplitude} \le 10^\circ$, $0 \le f \le 100$ Hz, (reduced frequency, $k = \pi fc/U_\infty = 0.15$ at $M_\infty = 0.5$). These are appropriate for the retreating blade flow over a helicopter. The tunnel is equipped with other necessary instrumentation.

The data was acquired using the real-time technique of Point Diffraction Interferometry (PDI). High quality interferograms were recorded as the airfoil shape was changed in both steady and oscillating airfoil flows at M_∞= 0.3. These were analyzed to recover the pressure distributions whenever the flow was attached and was shock-free. Otherwise, the images were used qualitatively.

III. RESULTS AND DISCUSSION

To prove the DDLE concept for controlling steady separated flows, the airfoil shape was varied from shape-0 to shape-22 for $8^\circ \le \alpha \le 18^\circ$ at $M_\infty = 0.3$. The PDI images were used to classify the flow as fully attached, attached with trailing edge separation, leading edge separated, etc. Fig. 2 (Ref. 5) shows that for some rounder nose shapes the static stall angle is increased at this Mach number. In fact, around shape-8, static stall is delayed to 18 deg. This improvement for the shape-8 airfoil is obtained by the reduced leading edge adverse pressure gradient realized from increasing the leading edge radius (Ref. 5). The fluid acceleration around the leading edge is reduced resulting in a decrease in the local gradients and hence, delay of stall onset. This expanded attached flow envelope provides a basis for defining the range of shape adaptation needed for dynamic stall control. It should be noted here that there is a delay in the development of the pressure field over an airfoil in unsteady flows. The "pressure lag" effect depends on the reduced frequency and can be exploited to achieve stall alleviation.

Figure 3 (Ref. 6) shows the shape adaptation schedule used along with the airfoil angle of attack variation when the airfoil was oscillated as $\alpha = 10^{\circ}+10^{\circ}\sin\omega t$. This case is referred to as the Shape Adapting while Pitching (SAP) airfoil. During each such deformation schedule, one phase-locked PDI image was recorded at a pre-selected angle of attack. The flow over fixed, shape DDLE airfoils was also studied to compare the effects of dynamic shape adaptation on dynamic stall control. The need for shape adaptation arises in a rotor blade because of the high-speed flight on the advancing side and the slower, high angle of attack flight on the retreating side.

The development of the peak suction over the NACA 0012, shape-8.5 and the SAP airfoils for $M_{\infty} = 0.3$, $k = 0.05$ is compared in Fig. 4 (Ref. 6). It shows that suction development over the two DDLE cases is delayed by about 2 degrees at lower angles of attack and by about 4 degrees at the higher ones. The abrupt loss of peak suction over the NACA 0012 airfoil indicates the occurrence of dynamic stall. On the other two airfoils, it is gradual even at high angles of attack, indicating trailing edge stall, a result borne out by the PDI pictures as well. For the DDLE cases, the recovery of the peak suction occurs at a higher angle of attack. Between the two DDLE cases studied, the SAP airfoil shows a smaller loop suggesting that its performance is better than that of the fixed shape-8.5 airfoil.

The vorticity flux over the two DDLE airfoils studied is plotted in Fig. 5 (Ref. 6). At the angles shown, the flow over the NACA 0012 airfoil (over which the peak vorticity levels is around 300, even at lower angles of attack) is in deep dynamic stall state. The maximum level seen in Fig. 5 is less than 150 proving that a 50% reduction was achieved using the DDLE concept enabling flow control. Thus, the vorticity did not coalesce and hence, no dynamic stall occurred and no vortex formed at this Mach number. The higher peak suction values and the flatter pressure distributions (Ref. 5) that were obtained for the DDLE airfoil lead one to believe that dynamic stall control was achieved without compromising the lift characteristics of the DDLE airfoil.

IV. CONCLUSIONS

Successful control of both steady and unsteady compressible flow separation over an airfoil was achieved using the concept of the DDLE airfoil. The airfoil enabled manipulation of the flow vorticity field by introducing **large** potential flow changes through **very small** leading edge modifications.

ACKNOWLEGDMENTS: This research was supported by the U.S. Army Research Office through a grant to the Naval Postgraduate School. The experiments were carried out in the Fluid Mechanics Laboratory at NASA Ames Research Center. The contributions of Dr. M.C.Wilder and Dr. L.W.Carr to this research are highly appreciated.

REFERENCES

[1] Carr LW, Progress in analysis and prediction of dynamic stall, J Aircraft, 1988, 25(1), 6-17.

[2] Chandrasekhara MS, Wilder MC, Carr, LW, Competing mechanisms of compressible dynamic stall, AIAA J, 1998, 36(3), 387-393.

[3] Reynolds WC, Carr LW, Review of unsteady, driven, separated flows, AIAA-85-0527, 1985.

[4] Chandrasekhara MS, Carr LW, Wilder MC, Sticht CD, Paulson GN, Design and development of a dynamically deforming leading edge airfoil for unsteady flow control, IEEE Publication 97CH36121, 1997, 132-140.

[5] Chandrasekhara MS, Wilder MC, Carr LW, Unsteady stall control using dynamically deforming airfoils, AIAA J, 1998, 36(10), 1792-2000.

[6] Chandrasekhara MS, Wilder MC, Carr LW, Compressible dynamic stall control using a shape adaptive airfoil, AIAA-99-0655, 1999.

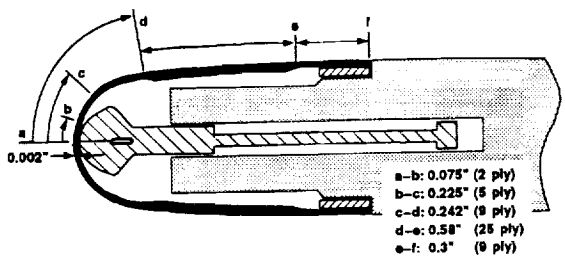

Fig. 1. Schematic of the DDLE design

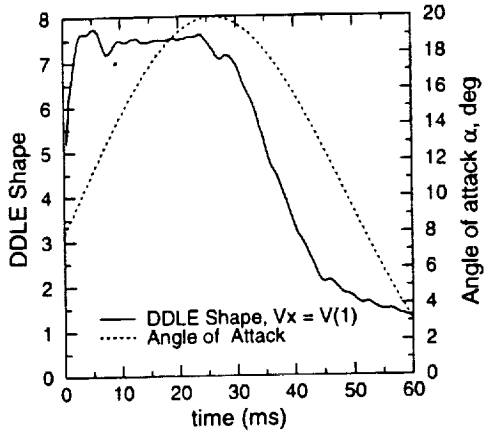

Fig. 3. Typical airfoil shape adaptation schedule

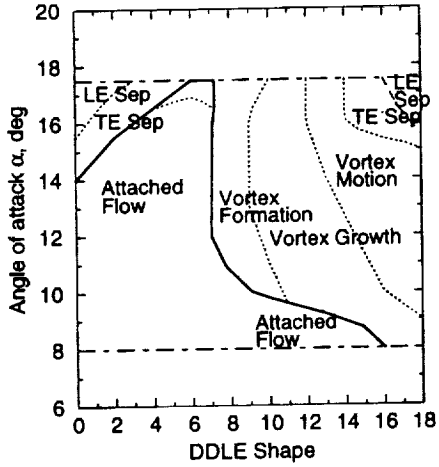

Fig. 2. DDLE airfoil flow regimes, M = 0.3, k = 0

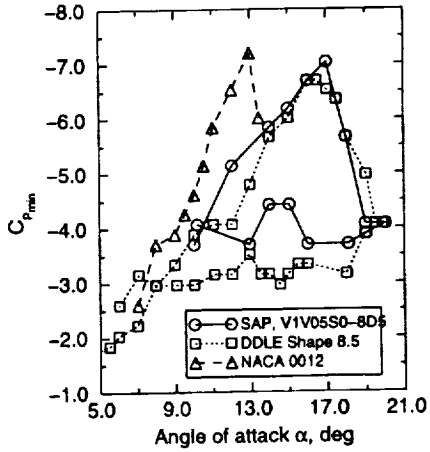

Fig. 4. Peak suction development over different airfoils, M = 0.3, k = 0.05

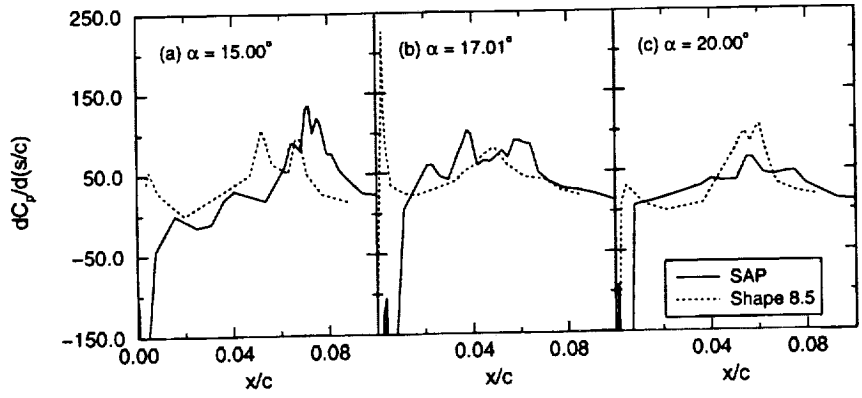

Fig. 5. Vorticity flux distribution over the DDLE airfoils, M = 0.3, k = 0.05